Carbohydrate Polymers 111 (2014) 830–840

Contents lists available at ScienceDirect

Carbohydrate Polymers

journal homepage: www.elsevier.com/locate/carbpol

Preparation and characterization of guar gum hydrogels as carrier materials for controlled protein drug delivery

Hiroyuki Kono*, Fumihiro Otaka, Masato Ozaki

Department of Science and Engineering for Materials, Tomakomai National College of Technology, Nishikioka 443, Tomakomai, Hokkaido 059 1275, Japan

ARTICLE INFO

Article history:
Received 25 March 2014
Received in revised form 25 April 2014
Accepted 8 May 2014
Available online 28 May 2014

Keywords:
Guar gum
Hydrogel swelling
Enzyme degradability
Protein adsorption
Protein release

ABSTRACT

Hydrogels were prepared from guar gum (GG) via esterification with 1,2,3,4-butanetetracarboxylic dianhydride (BTCA). Detailed spectroscopic analysis using FTIR and solid-state NMR revealed that an increase in the BTCA feed amount in the preparation mixture led to an increased degree of crosslinking, which affected the swelling behavior and rheological properties of the hydrogels. The hydrogels exhibited enzyme degradability, and after incubation with β-mannanase and α-galactosidase, 30–57% of the hydrogels were degraded. In addition, the hydrogels adsorbed bovine serum albumin and hen egg white lysozyme thorough electrostatic and hydrophobic interactions. The protein-adsorbed GG hydrogels exhibited a slow and steady release of the proteins over a 24 h period in buffer solutions after a fast release of proteins in the first hour. As such, GG hydrogels are expected to be efficient drug delivery carriers for protein-based drugs.

1. Introduction

The application of natural polysaccharides is becoming more and more important due to their low environmental impact and nontoxicity to humans. Especially, polysaccharide-based hydrogels have aroused much interest in pharmaceutical field as carriers for drugs, 3D scaffolds for cell culture, fillers for tissue engineering, and so on (Coviello, Matricardi, Marianecci, & Abaique, 2007). The chemical crosslinking between polysaccharide chains allow the obtainment of compounds in a wide range of pH with a good mechanical stability (Brandl, Sommer, & Goepferic, 2007).

Guar gum (GG), which can be obtained from the seed of the legume *Cyamopsis tetragonalobus*, is a functional polysaccharide composed of a linear chain of D-mannose residues (Man) connected by (1→4)-β-glycosidic linkages. Pendant from the Man backbone are D-galactose residues (Gal) attached via (1→6)-α-glycosidic linkage units. Recent experiments using enzyme degradation (Gamal-Eldeen, Amer, & Helmy, 2006) and spectroscopic methods (Crescenzi et al., 2004) revealed the random distribution of Gal side groups and a Man-to-Gal ratio of ca. 1.6–1.8:1. Among naturally occurring water-soluble polysaccharides, GG is known to have one of the highest molecular weights (Mw), in the vicinity of $\sim 2.8 \times 10^7$ g mol^{-1} (Barth & Smith, 1981; Vijayendran & Bone, 1984). Due to its low cost, nontoxicity, biodegradability, biocompatibility, high viscosity, and high water-solubility, GG is now used in many industries (Cui, Mazza, & Biliaderis, 1994): as sizing and finishing agents in the textile and paper industries; as a binder, stabilizer, and thickener in the cosmetics and food industries; and as a fracturing fluid additive in mining and hydraulic fracturing processes (Chudzikowski, 1971; Wang, Ellis, & Ross-Murphy, 2000). In the pharmaceutical sector, its functional properties are of primary importance for controlling the release of drugs in the gastrointestinal tract, such as, as a carrier for colon targeted drugs (Das, Wadhwa, & Srivastava, 2006), for anticancer drugs in the treatment of colorectal cancer (Chaurasia et al., 2006), and for oral rehydration solutions in the treatment of cholera in adults (Alam et al., 2000). The chemical crosslinking of GG has been performed with glutaraldehyde (Gliko-Kabir, Yagen, Penhasi, & Rubinstein, 1998) and phosphating agents (Gliko-Kabir, Yagen, Penhasi, & Rubinstein, 2000a; Gliko-Kabir, Yagen, Penhasi, & Rubinstein, 2000b) or in combination with polyacrylic acid (Abo-Shosha, Ibrahim, Allam, & El-Zairy, 2008), in order to obtain polyelectrolyte hydrogels with

Abbreviations: BBO, broad band observe; BSA, bovine serum albumin; BTCA, 1,2,3,4-butanetetracarboxylic dianhydride; DDMAS, dipolar-decoupled/magic angle spinning; DMAP, 4-dimethylaminopyridine; DNS, dinitrosalicylic acid; DSS, 4,4-dimethyl-4-silapentane-1-sulfonic acid; D_2O, deuterium oxide; EDTA, ethylenediamine tetraacetic acid; FTIR, Fourier transform infrared spectroscopy; G′, storage modulus; G″, loss modulus; Gal, D-galactose residue; GG, guar gum; Man, D-mannose residue; MAS, magic angle spinning; NAD^+, nicotinamide adenine dinucleotide; NMR, nuclear magnetic resonance; PBS, phosphate buffered salt; p*I*, isoelectric point; pK_a, acidity constant; SPINAL64, small phase incremental alternation with 64 steps; SR, swelling ratio.

* Corresponding author. Tel.: +81 144 67 8036; fax: +81 144 67 8036.
E-mail address: kono@sem.tomakomai-ct.ac.jp (H. Kono).

http://dx.doi.org/10.1016/j.carbpol.2014.05.050
0144-8617/

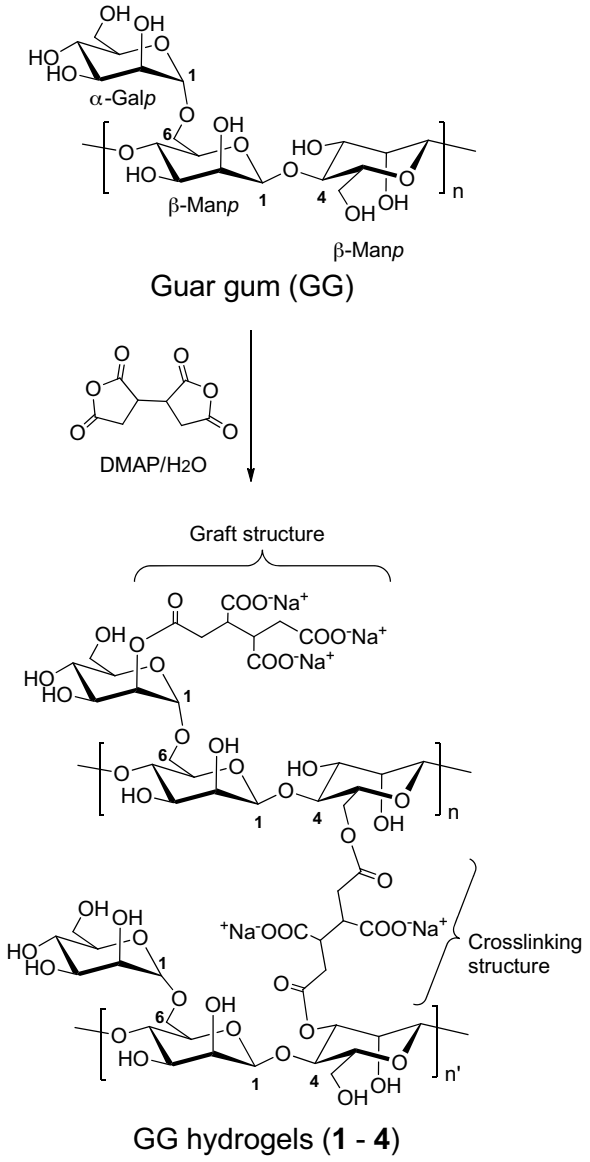

Fig. 1. GG hydrogel synthesis via crosslinking of GG with BTCA. Crosslinking and grafting reaction by BTCA could possibly occur at any hydroxyl group of GG, and the possibility was omitted in this figure.

mouldable mechanical properties, swelling degree, and controlled drug release characteristics.

The aim of this study is the synthesis of a new GG-based hydrogels using 1,2,3,4-butanetetracarboxylic dianhydride (BTCA) as a crosslinking agent (Fig. 1). BTCA contains two acid anhydrides in its structure, and each readily reacts with certain functional groups such as isocyanates, amines, and hydroxyl groups to undergo crosslinking. With polysaccharides such as cellulose and chitin, two free carboxyl acid groups are formed with simultaneous esterification and/or amidation crosslinking with the hydroxyl and/or primary amino groups of the polysaccharide chains (Kono & Fujita, 2012; Kono, Fujita, & Oeda, 2013; Kono & Zakimi, 2013). Thus, the merit of the BTCA is to convert nonionic polysaccharides to the chemically crosslinked anionic hydrogels by one-step reaction. In addition, it was revealed that The BTCA-crosslinked polysaccharides exhibited varying phase transitions in response to changes in external pH conditions because of their anionic groups (Kono & Fujita, 2012; Kono, Fujita, et al., 2013). Thus, these hydrogels crosslinked by BTCA might act as potential matrices for the loading of proteins or other hydrophilic bioactive drugs in drug delivery systems.

Here, we present the preparation of GG-based hydrogels via the reaction of GG with BTCA in an aqueous medium containing 4-dimethylaminopyridine (DMAP) as an esterification catalyst. By changing the feed amount of BTCA to GG, we prepared a series of GG hydrogels and characterized the structures of the hydrogels using Fourier transform infra-red (FTIR) and solid-state ^{13}C nuclear magnetic resonance (NMR) spectroscopies. This article also describes the water absorbency, rheological properties, and enzymatic degradability of the hydrogels. In addition, the protein adsorption and release abilities of the GG hydrogels were characterized using egg white lysozyme and BSA to estimate their potential as a carrier material for protein drugs. By investigating the effect of pH and ionic strength of the protein-adsorption medium, the interactions between the GG hydrogel and the proteins were characterized.

2. Experimental

2.1. Materials

Highly purified and finely powdered GG (CP-Kelco Supergel CSA200/50 whose viscometric average molecular weight is 2.6×10^5 g mol^{-1}) was provided by Sansyo Co. Ltd., Japan. GG was used without further purification. BTCA was supplied by Shin Nippon Rika Co. Ltd., Japan. A phosphate buffered salt (PBS) tablet (pH 7.4) was purchased from Takara Bio Inc., Japan. A galactomannan assay kit was purchased from Megazyme International Ireland Ltd. The assay kit contained a suspension of *Aspergillus niger* β-mannanase (350 U mL^{-1}), guar seed α-galactosidase (450 U mL^{-1}), *A. niger* β-mannanase (350 U mL^{-1}), *Pseudomonas fluorescens* β-galactose dehydrogenase (420 U mL^{-1}), 1 M nicotinamide adenine dinucleotide (NAD^+), 2 M Tris–HCl buffer (pH 8.6) containing 1 mM EDTA, and a D-galactose standard solution (0.4 g L^{-1}) containing 0.02% sodium azide. The kit was used for the enzyme-degradability tests. Egg white lysozyme and BSA were purchased from Wako Pure Chemicals Co. Japan. All other reagents used in this study were of analytical grade and were purchased from Kanto Chemicals, Japan.

2.2. Preparation of GG hydrogels

Four GG hydrogels (samples **1**–**4**) were prepared from GG and BTCA. A typical procedure included the following: GG (1.0 g, 2.3 mmol for average repeating unit) was completely dissolved in 100 mL deionized water containing DMAP (2.44 g, 20 mmol) via stirring with a Teflon impeller at 300 rpm at room temperature. After complete dissolution of GG, BTCA (0.80 g, 4.0 mmol) was added with stirring at 300 rpm. Esterification proceeded with stirring at room temperature for 24 h, after which the reaction mixture was poured into a solution of 1:1 (v/v) ethanol and water (500 mL) to precipitate the product. The product was neutralized (pH 7.0) with 10% (w/v) aqueous NaOH by monitoring with a pH electrode. The precipitate was filtered using a glass filter and was purified twice by precipitation with 1:1 (v/v) ethanol and water. The purified product was dried under reduced pressure to obtain a white granular GG hydrogel (sample **1**). Using a similar method, the other GG hydrogels (samples **2**–**4**) were prepared. The amounts of GG and BTCA used for the preparation of the GG hydrogels are listed in Table 1. All GG hydrogels were stored in a desiccator under vacuum until use.

Table 1
Reaction conditions and yields of GG hydrogels (samples **1**–**4**).

Sample	Initial additive amounts during preparation		Yields[a]
	GG	BTCA	
1	1.0 g(2.3 mmol)	0.8 g(4.0 mmol)	0.96 g(92%)
2	1.0 g(2.3 mmol)	2.0 g(10 mmol)	0.98 g(93%)
3	1.0 g(2.3 mmol)	3.0 g(15 mmol)	0.99 g(90%)
4	1.0 g(2.3 mmol)	4.0 g(20 mmol)	1.14 g(90%)

[a] Yield (%) of each sample was calculated using the following equation: Yield (%) = [(mass of each hydrogel/g)/(Mw of the average repeating unit of each hydrogel/g mmol^{-1})] × 100/2.3 mmol. The Mw of the average repeating unit of each hydrogel is shown in Table 3.

2.3. Structural characterization

2.3.1. FTIR spectroscopy

FTIR spectra were measured using a PerkinElmer Spectrum Two spectrometer (PerkinElmer Inc., US). All samples were analyzed as KBr pellets, prepared by blending 2 mg of the powdered polymer with 100 mg of KBr that was previously dried at 105 °C for 24 h. The FTIR spectra were obtained at a spectral resolution of 1 cm^{-1} by the accumulation of 16 scans within the frequency range of 4000–500 cm^{-1}.

2.3.2. NMR spectroscopy

All NMR spectra were recorded on an AVIII spectrometer (Bruker BioSpin GmbH, Germany, 500.13 MHz for ^{1}H and 125.13 MHz for ^{13}C). Solution-state NMR spectra of GG were obtained using a 2-channel 5 mm broad band observe (BBO) probe incorporating a *z*-gradient coil. The measurement temperature was set to 300 K. For the NMR experiments, GG (3 mg) was dissolved in 600 μL of D_2O in a 5 mm NMR glass tube (Wilmad-Labglass Co., US). For quantitative discussions, inverse-gated ^{1}H-decoupled ^{13}C NMR spectra (Canet, 1976) were recorded using the Bruker Biospin pulse program. ^{13}C excitation pulse with a flip angle of 30°, data acquisition time, and repetition time were set to 10 μs, 2.7 s, and 30 s, respectively. Five thousand scans were collected. ^{1}H and ^{13}C chemical shifts were calibrated by assigning the methyl peak of DSS as 0 ppm.

Solid-state dipolar-decoupled/magic angle spinning (DDMAS) ^{13}C NMR spectra were recorded at 25 °C with a 4 mm dual-tuned MAS probe at a MAS frequency of 12.5 kHz. The ^{13}C excitation pulse length (flip angle of 30°), data acquisition time, and repetition time were set to 1.35 μs, 15 ms, and 20 s, respectively. During the data acquisition period, small-phase incremental alternations with a 64 step (SPINAL 64) decoupling sequence (Fung, Khitrin, & Ermolaev, 2000) and a ^{1}H field strength of 75 kHz were applied to ^{1}H nuclei. The spectra were typically accumulated with 4096 or 5120 scans. ^{13}C chemical shifts of the DDMAS spectra were calibrated based on the carbonyl carbon resonance of D-glycine at 176.03 ppm, which was used as an external reference. The lineshape analysis of the DDMAS ^{13}C NMR spectra was performed using the solid-lineshape tool of the Bruker BioSpin TopSpin software package (Ver. 3.0), and the nonlinear least squares method was employed for the lineshape analysis using the Gauss–Lorentz functions, as described previously (Kono, Erata, & Takai, 2002; Kono & Fujita, 2012; Kono, Yunoki, et al., 2002).

2.4. Rheological properties

Each GG hydrogel (100 mg) was swollen in 2 mL PBS buffer (pH 7.4) at 4 °C for 24 h, and the swollen hydrogels were used for the rheological measurements. The rheological behavior of the swollen hydrogels was evaluated in triplicate using a Physica MCR 301 rheometer (Anton Paar GmbH, Austria) equipped with a Rheoplus 32 data analyzer and fitted with a Peltier temperature control. A 25 mm rough surface cone-plate measuring geometry was used to prevent sample slippage. The temperature of all measurements was 298 K. The gap and stain were set at 1.0 mm and 1.0%, respectively. Oscillatory share responses (G′ or storage modulus and G″ or loss modulus) were determined at 0.1 Pa over the frequency range. Steady shear tests were performed over a share rate range of 0.1–100 rad s^{-1} (Kono, 2014). The test conditions were within the linearity range of the viscoelastic properties.

2.5. Swelling behavior

Dried GG hydrogel (ca. 100 mg) was precisely weighed and placed into a 15 mL polypropylene centrifuge tube. The desired solutions were poured into the tube and the temperature of the tube was set at 25 °C. After 24 h, the tube was centrifuged at 8000 × *g* for 5 min, and the supernatant was drained. The swelling ratio (SR) was determined using Eq. (1),

$$SR = \frac{W_s - W_d}{W_d} \quad (1)$$

where W_s is weight of the swollen GG hydrogels and W_d is the weight of the dried GG hydrogel. As external solutions for determining the SR, 20 mM HCl–KCl (pH 2), 20 mM citric acid–sodium citrate (pH 3–6), 20 mM NaH_2PO_4–Na_2HPO_4 (pH 7–8), 20 mM Tris–HCl (pH 9), 20 mM $NaHCO_3$–NaOH (pH 10–11), and KCl–NaOH (pH 12) were used. The SR was measured for four samples of each GG hydrogel, and the average of the four values was plotted against the pH of the buffer. In addition, the effect of ionic strength on the SR of each hydrogel was investigated using 20 mM NaH_2PO_4–Na_2HPO_4 (pH 7) buffer containing NaCl. The NaCl concentration was set to 0–1.5%.

2.6. Enzymatic degradability

The enzymatic degradability of GG and GG hydrogels was investigated using a galactomannan assay kit. The procedure was performed in accordance with the provided protocol. Briefly, GG or GG hydrogel was milled to pass a 20-mesh screen using a PLC-2M plastic cutting mill (Osaka Chemical Co., Japan). Approximately 100 mg of the sample was weighed into a 15 mL polypropylene centrifuge tube and 8 mL 100 mM sodium acetate buffer (pH 4.5) was added. After complete dissolution of GG or complete swelling of GG hydrogels, 10 μL of *A. niger* β-mannanase was added to the tube. The tube was vigorously mixed via vortex for 30 s and then shaken for 60 min at a rate of 120 rpm on a shaker set at 40 °C. The solution in the tube was diluted with water to 25 mL and the contents were thoroughly mixed. To a 1.5 mL microtube, 200 μL of the flask solution, 100 μL of 10 mM acetate buffer (pH 4.5), and 20 μL of guar seed α-galactosidase plus *A. niger* β-mannanase suspension were added, and the mixture was incubated at 40 °C. After 60 min of incubation, the mixture was separated into two aliquots. The amount of the liberated total reducing sugars in the mixture which contained Gal, Man, and manno-oligosaccharides was determined by the dinitrosalicylic acid (DNS) method (Miller, Blum, Glennon, & Burton, 1960). The amount of Gal liberated from GG or GG hydrogels was determined using the other aliquot. Briefly, the aliquot (150 μL) was added to a 2 mL microtube and 1 mL of distilled water, 200 μL of 2 M Tris–HCl buffer (pH 8.6) containing 1 mM EDTA, and 100 μL of NAD^+ solution were added. After 3 min, 20 μL of β-galactose dehydrogenase was added and the tube was incubated at room temperature for 40 min. The concentration of D-galactose was indirectly estimated by the amount of NADH in the solution (Pettersson, & Pettersson, 2001). The NADH concentration was determined at 340 nm using an Epoch 96 well micro-volume spectrophotometer (BioTek Instruments, Inc., US) and a 96 well quartz microplate (Hellma GmbH, Germany). The amounts of total reducing sugars and D-galactose were determined by the calibration curves made

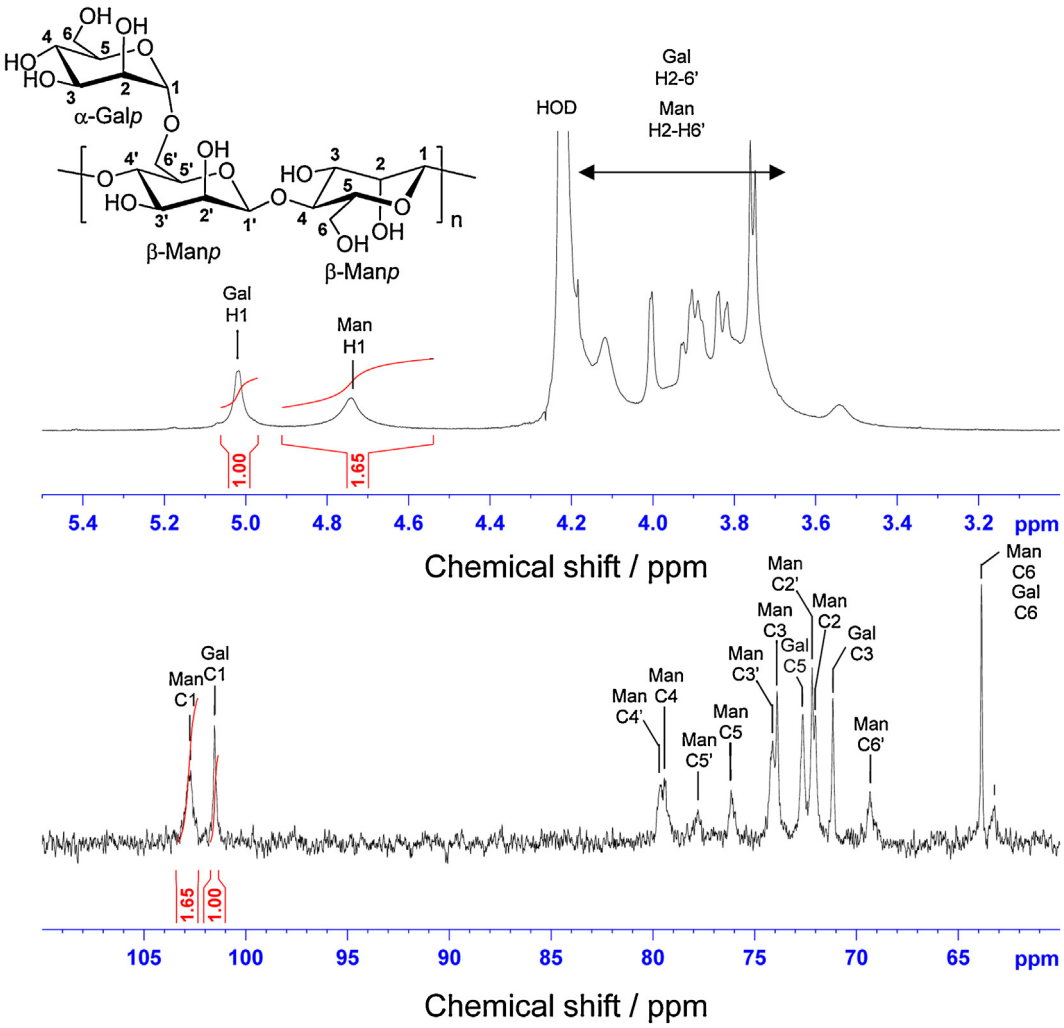

Fig. 2. ^{1}H and quantitative ^{13}C NMR spectrum of GG in D_2O at 300 K. ^{1}H and ^{13}C resonance assignment of GG is also shown in these spectra, and ^{1}H and ^{13}C atoms of Man residues with branch points from 6-position linked to Gal were designated by prime notations.

using the galactose standard solution of the galactomannan assay kit.

2.7. Protein adsorption and release

The effects of adsorption time, pH of the adsorption medium, and initial protein concentration on the adsorption capacity of the GG hydrogel (sample **4**) were studied using lysozyme and BSA as model proteins. The time dependency of the protein adsorption was investigated by dissolving 30 mg of each protein in 30 mL of 20 mM NaH_2PO_4–Na_2HPO_4 buffer (pH 7) in a 50 mL polypropylene centrifuge tube. GG hydrogel (30 mg; sample **4**) was precisely weighed and added to the protein-containing buffer. The adsorption experiments were then conducted on a shaker set at 40 °C with a shaking rate of 120 rpm. After a prescribed period of time, an aliquot (500 μL) was withdrawn from the mixture. The mixture was immediately centrifuged at 15,000 rpm for 2 min, and the protein concentration of the supernatant was estimated at 280 nm using an Epoch 96 well micro-volume spectrophotometer and a 96 well quartz microplate. The amount of protein adsorbed to the hydrogels was determined by Eq. (2):

$$\text{Protein adsorption}\ (\%) = \{[\text{Protein}]_{\text{init}} - [\text{Protein}]_{\text{sup}}\} \times \frac{100}{[\text{Protein}]_{\text{init}}} \quad (2)$$

where $[\text{Protein}]_{\text{init}}$ and $[\text{Protein}]_{\text{sup}}$ are the initial protein concentration of buffer solution and the protein concentration of supernatant after protein adsorption, respectively. The dependency of the pH of the adsorption medium and initial protein concentration on the protein adsorption capacity of the GG hydrogels was determined by a procedure similar to that used to determine the time-dependency of the protein adsorption capacity. The adsorption time was set to 24 h for these experiments. The pH of the adsorption medium was varied from 2 to 12 using various buffer systems including 20 mM HCl–KCl (pH 2), 20 mM citric acid–sodium citrate (pH 3–6), 20 mM NaH_2PO_4–Na_2HPO_4 (pH 7–8), 20 mM Tris–HCl (pH 9), 20 mM $NaHCO_3$–NaOH (pH 10–11), and KCl–NaOH (pH 12). The initial protein concentration in the adsorption medium ranged from 0.5 to 5 mg mL^{-1}.

The protein-adsorbed GG hydrogels were freeze-dried, and the resulting hydrogels were used for the protein release experiments. Freeze-dried hydrogel (30 mg) was added to a 50 mL polypropylene centrifuge tube containing 30 mL PBS (pH 7.4) or 20 mM HCl–KCl buffer (pH 2). The tube was shaken at a rate of 120 rpm on a shaker set at 37 °C. After a prescribed period of time, an aliquot (500 μL) was withdrawn from the mixture. The mixture was immediately centrifuged at 15,000 rpm for 2 min, and the protein concentration of the supernatant was estimated at 280 nm. The protein release from the hydrogels was determined by applying the amounts of released and adsorbed protein

given in Eq. (3):

$$\text{Protein release}\ (\%) = (\text{the amount of released protein}) \times \frac{100}{(\text{the amount of adsorbed protein})} \quad (3)$$

3. Results and discussion

3.1. Man/Gal composition of GG

Fig. 2 shows the ^{1}H and the quantitative ^{13}C NMR spectra of GG and the ^{1}H and ^{13}C resonance assignments of Gal residues and Man residues with and without branch points from the 6-position linked to Gal (Chaubey, & Kapoor, 2001; Cunha, Vieira, Arriaga, de Paula, & Feitosa, 2009). In the ^{1}H NMR spectrum, H1 resonance of the two kinds of Man residues overlapped at 4.74 ppm, and the H1 of Gal appeared at 5.02 ppm. The peak integration of the resonance at 4.74 and 5.02 ppm provided the ratio of Man to Gal residues (Man/Gal) in the GG structure, specifically 1.65. This value was confirmed by the integral values of anomeric carbon resonance at 101.4 and 103.0 ppm due to the C1 of Gal and overlap of C1 of the Man residues, respectively. Hence, the molecular mass of the average repeating unit in GG, which contains 1.65 Man residues and 1Gal residue, was calculated to be 429 g mol^{-1}.

3.2. Preparation of GG hydrogels

A series of GG hydrogels (samples **1**–**4**) was prepared from GG by varying the BTCA feed amount to the average repeating unit of GG (Table 1). Immediately following the crosslinking reaction with BTCA, GG become increasingly viscous, transforming from a solution into a gel at approximately 30–60 min after the initial reaction. The crosslinking reaction proceeded with stirring at room temperature for 24 h, and the resulting product was neutralized, purified, and dried under reduced pressure. The dried GG hydrogels were granular, white powders and the yields were in the range of 90–93% (Table 1).

3.3. Structural characterization

3.3.1. FTIR spectra

Fig. 3 shows the FTIR spectra of GG and GG hydrogels (samples **1**–**4**). Following the crosslinking of GG with BTCA, the obtained GG hydrogels showed several new absorption bands in addition to the original GG bands. The new absorption bands at 1728, 1593, and 1402 cm^{-1} were assigned to the C=O stretching vibration of the ester, and the C=O asymmetric and symmetric stretching vibration of the carboxylate anion, respectively (Kono & Fujita, 2012; Kono & Zakimi, 2013). The band at 1648 cm^{-1} arose from the bending vibration of water molecules adsorbed in each sample during KBr disk preparation (Kono & Fujita, 2012). The intensity of the bands at 1728, 1593, and 1402 cm^{-1} increased with the sample number. This indicated that the hydroxyl groups of GG were esterified with BTCA, resulting in the formation of sodium carboxylate groups as well as the esterification between GG chains. Moreover, the amount of BTCA esterified with GG increased with the initial feed amount of BTCA to GG in the preparation of the hydrogels.

3.3.2. Solid-state ^{13}C NMR spectra

Fig. 4 shows the solid-state DDMAS ^{13}C NMR spectra of GG and GG hydrogels (sample **1**–**4**), and the individual fit lines for the spectra of GG hydrogels determined by the nonlinear least-squares line-fitting method. Peaks at 101, 80, 72, and 61 ppm were observed in the spectrum of GG. The resonance at 101 ppm was assigned to the C1 resonance of Gal and Man residues, the signal

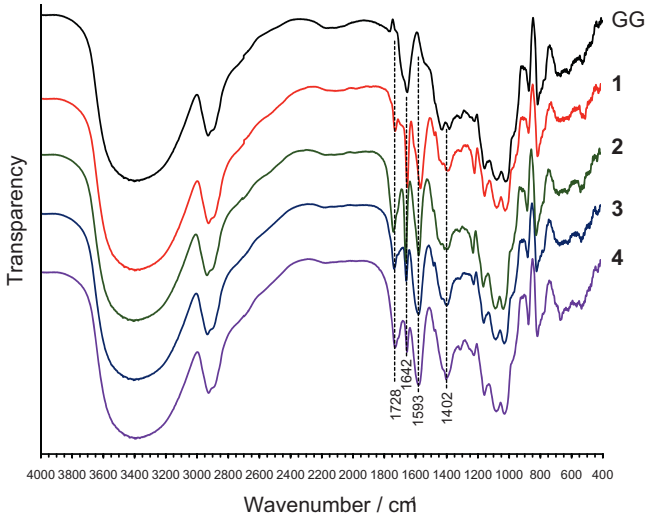

Fig. 3. FTIR spectra of GG and GG hydrogels (samples **1**–**4**). The bold number in the right of the spectra indicates the sample number.

at 61 ppm was due to the C6 of these residues, and the signals at 80 and 72 ppm were due to the other carbons (Chaubey & Kapoor, 2001; Cunha et al., 2009; Parvathy, Susheelamma, Tharanathan, & Gaonkar, 2005). In the case of the GG hydrogels, the spectra were deconvoluted to 8 signals and the signals at 101, 80, 72, and 61 ppm were attributed to the carbons of Man and Gal residues. The new four signals at 182, 175, 48 and 41 ppm should be associated with carbons of BTCA reacted with GG and could be assigned to the carbonyl carbons of ester bonds, those of the sodium carboxylate group, methylene carbons, and methyne carbons (Kono & Fujira, 2012; Kono, Fujita, et al., 2013; Kono, Oeda, & Nakamura, 2013). This clearly indicated that the esterification occurred between the anhydride of BTCA and the hydroxyl groups of GG and that free carboxylate groups were simultaneously generated from the acid anhydride of BTCA.

Based on the lineshape analysis of the NMR spectra, the structures of the GG hydrogels were characterized. Tri- or tetra-linkages derived from the ester linkages between the hydroxyl group of GG and the newly formed carboxyl group in BTCA resulting from the grafting or crosslinking with another GG molecule, were also accounted for during the reaction. However, the formation of tri- and tetra-linkages occurs to a much lesser extent than mono- and di-linkages because acylations of hydroxyl groups by acid anhydrides are more efficient than the reaction with the carboxylate group (Kono, Oeda, et al., 2013; Xu et al., 2005). Therefore, tri- and tetra-linkages were not favored under the mild conditions used for the reaction. Table 2 summarizes the integral values of the ^{13}C resonance lines with the peaks of 182, 175, 101, 48, and 41 ppm (I_{acid}, I_{ester}, I_{C1}, I_{CH}, and I_{CH2}, respectively) when I_{C1} was set to 1 for all spectra. Initially, the average number of total, crosslinked, and grafted BTCA molecules per average repeating unit of GG containing 1.65 Man and 1Gal residues were set to n_{BTCA}, n_C, and n_G, respectively. In addition, as shown in Fig. 1, one diester and two carboxylic acid species formed during crosslinking, whereas the graft reaction resulted in the formation of one ester and three carboxylic acids. Therefore, n_{BTCA}, n_C, and n_G were determined by Eqs. (4)–(6).

$$n_{BTCA} = n_C + n_G = \frac{I_{acid} + I_{ester}}{4} \quad (4)$$

$$n_C = \frac{3I_{ester} - I_{acid}}{4} \quad (5)$$

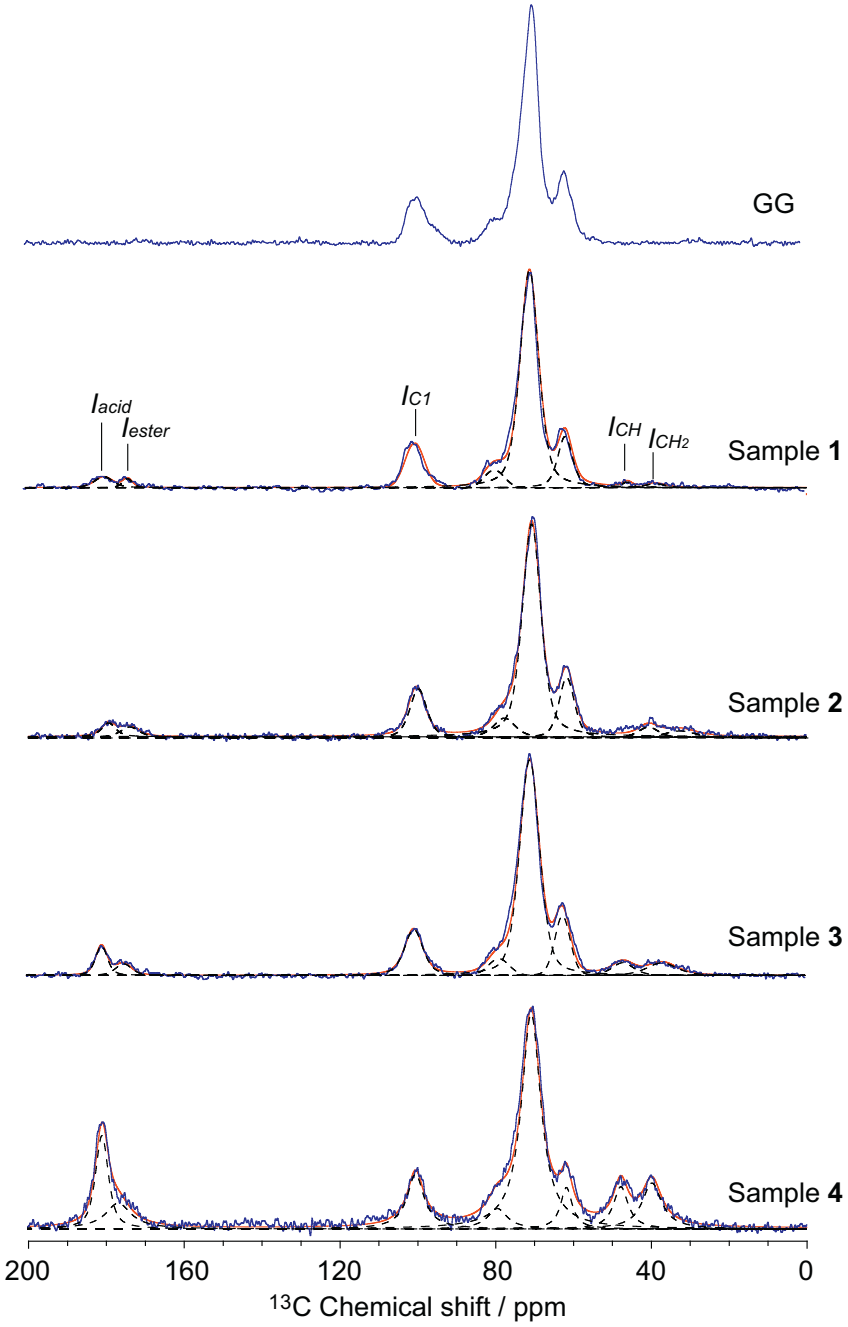

Fig. 4. Solid-state DDMAS ^{13}C NMR spectra of GG and GG hydrogels (samples **1**–**4**). Individual fit lines are indicated by dotted lines in the spectra of GG hydrogels and are determined by the lineshape analysis shown in this figure. Synthetic spectrum formed by the fit lines for each sample is shown by the red line. Integral values for the individual fit lines for peaks at 182, 175, 48, and 41 ppm due to the carbonyl carbons of sodium carboxylate group, ester carbon, methyne carbon, and methylene carbons, are denoted as I_{acid}, I_{ester}, I_{CH}, and I_{CH2}, respectively, and are summarized in Table 2. For each spectra, I_{C1}, the integral value for the line at 101 ppm assigned to the anomeric carbons of GG, was set to 1.

$$n_G = \frac{2I_{acid} - 2I_{ester}}{4} \quad (6)$$

Thus, the percentage of crosslinked and grafted BTCA molecules could be determined using Eqs. (7) and (8).

$$(\text{Crosslinked BTCA}) \quad \% = n_C \times \frac{100}{n_{BTCA}} \quad (7)$$

$$(\text{Grafted BTCA}) \quad \% = n_G \times \frac{100}{n_{BTCA}} \quad (8)$$

The structural parameters n_{BTCA}, n_G, and n_C determined by Eqs. (4)–(6) and the percentage of crosslinked and grafted BTCA determined by Eqs. (7) and (8) are summarized in Table 2. Based on the structural data, n_{BTCA} increased with increased feed amounts of BTCA in the preparation mixture. In addition, the graft reaction increased gradually with increasing BTCA feed amounts, although the crosslinking density (n_C) was enhanced with increased BTCA feed amounts. The difference in the grafting and crosslinking proportion at a low concentration of BTCA was because crosslinking with BTCA is a two-step reaction, whereas grafting is a single-step process (Kono & Fujita, 2012). The initial step in the crosslinking involves the attack of an acid anhydride in BTCA by a hydroxyl group, after which another acid anhydride within the same BTCA molecule attaches to another hydroxyl group. At high BTCA

Table 2
Result of the lineshape analysis and structural data of the GG hydrogels (samples **1**–**4**).

Sample	I_{acid} [a]	I_{ester} [a]	I_{C1} [a]	I_{CH} [a]	I_{CH2} [a]	n_{BTCA} [b]	n_C [c] (Crosslinked BTCA %)	n_G [c] (Grafted BTCA %)
1	0.16	0.15	1	0.13	0.14	0.08	0.075 (94%)	0.005 (6%)
2	0.22	0.18	1	0.19	0.23	0.10	0.080 (80%)	0.020 (20%)
3	0.38	0.27	1	0.30	0.32	0.16	0.11 (66%)	0.054 (34%)
4	1.06	0.65	1	0.86	0.84	0.43	0.22 (52%)	0.21 (48%)

[a] I_{acid}, I_{ester}, I_{CH}, and I_{CH2} are the integral value of the Gauss–Lorentzian lines with peaks at 182, 175, 48, and 41 ppm, respectively. These lines are due to the carbonyl carbons of the sodium carboxylate group, ester carbon, methyne carbon, and methylene carbons in each solid-state DDMAS ^{13}C NMR spectrum shown in Fig. 4, respectively. For all samples, I_{C1} corresponded to the Gauss–Lorentzian line for the anomeric carbons of GG and was set to 1.
[b] Average number of the total reacted BTCA molecules per the average repeating unit of each GG hydrogel.
[c] n_C and n_G are average number of crosslinked and grafted BTCA molecules per average repeating unit of each hydrogel, respectively. Thus, the sum of n_C and n_G equals n_{BTCA} in each GG hydrogel.

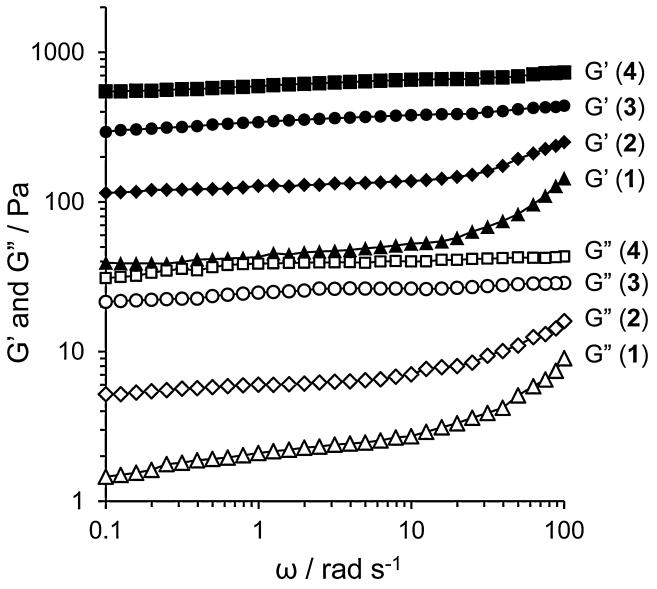

Fig. 5. Viscoelastic behavior of GG hydrogels (samples **1**–**4**, 100 mg) swollen with PBS buffer, pH 7.4 (2 mL) at 298 K.

concentrations, one acid anhydride group of BTCA is attacked by the hydroxyl group of GG, resulting in the formation of the graft structure. Consequently, the number of unreacted hydroxyl groups becomes relatively low and the steric-bulk of the GG chains is increased by grafting, which interferes with the crosslinking of other unreacted acid anhydrides within the BTCA molecule grafted onto GG. In contrast, with low BTCA concentrations, the acid anhydride group of BTCA that grafts onto GG is believed to react easily with other hydroxyl groups because the number of grafted BTCAs is relatively low as compared to that at a high BTCA concentration.

3.4. Rheological properties

The storage modulus (G′) and loss (G″) modulus of GG hydrogels as a function of ω between 0.1 and 100 rad s^{-1} are shown in Fig. 5. Samples **1**–**4** exhibited similar tendencies during the angular frequency sweeps. G′ was always higher than G″ and there was no cross-over points for the GG hydrogels, indicating that the GG hydrogels had characteristic gel structures (Bhattarai, Ramay, Gunn, Matsen, & Zhang, 2005). The G′ of samples **3** and **4** exhibited almost no dependence with the frequency characteristic of a permanent gel network. On the other hand, the G′ of samples **1** and **2** showed a drastic change in the frequency dependence over 10 rad s^{-1}, indicating that samples **1** and **2** exhibited the viscoelastic behavior of weak gels (Argüelles-Monal, Goycoolea, Peniche, & Higuera-Ciapara, 1998). As such, the viscoelastic behavior of the GG hydrogels strongly depended on the crosslinking degree n_C, as confirmed by the G″ values (Kono, 2014). With ω from 0.1 to 100 rad s^{-1}, G″ increased 1.33-fold for sample **1** and 1.36-fold for sample **2**. On the other hand, G″ increased 3.08-fold for sample **3** and 6.18-fold for sample **4**.

3.5. Swelling behavior

The white-colored granular GG hydrogels absorbed water readily and formed transparent hydrogels upon soaking. The water absorbency of the GG hydrogels gradually increased over time and reached equilibrium within 12 h (data not shown). Thus, the swelling ratio after 24 h of swelling was defined as the equilibrium SR. Fig. 6(A) shows the effect of the pH on the SR of the GG hydrogels. The SR of all hydrogels increased markedly with increased pH values because of the presence of carboxylate anions or carboxylic acids in the hydrogel structure. In acidic medium, the carboxyl groups of GG hydrogels were protonated yielding carboxylic acids, and the ionic repulsion disappeared, resulting in the shrinkage of the hydrogels. In neutral and alkaline media, the dominant species in the GG hydrogels were carboxylate anions, and the hydrogels were swollen due to intra-ionic repulsion between carboxylate anions. The acute change in the SR of the GG hydrogels (samples **2**–**4**) between pH 4 and 5 suggested that the pK_a values of the carboxylic acids in the hydrogels were around 4–5, which almost corresponded to the pK_a of 1,2,3,4-butanetetracarboxylic acid (pK_a = 4.2, Leenheer, Wershaw, & Reddy, 1995). For hydrogel **1**, the change in SR was ambiguous because the n_{BTCA} value of the sample was very low. The SR of the hydrogels in neutral and alkaline solutions increased with increased n_C up to sample **3**, while the SR of sample **4** was markedly lower. Thus, the optimal structure for water adsorption was sample **3** in neutral and alkaline solutions and the expansion of sample **4** was suppressed because of the high degree of crosslinking.

Fig. 6(B) shows the effect of the NaCl concentration on the SR of the GG hydrogels. All hydrogels showed a similar trend: the SR of the hydrogels gradually decreased with increased ionic strengths. At high NaCl concentrations, there was a difference between the concentration of the NaCl solution and that inside the GG hydrogel, which created a reduced osmotic pressure (Kono & Fujita, 2012), thereby lowering the absorbency of the hydrogels. The decreased SR with 0–1.5% NaCl was notable for samples **3** and **4**, indicating that the sodium carboxylate content in these hydrogels was higher than in samples **1** and **2**.

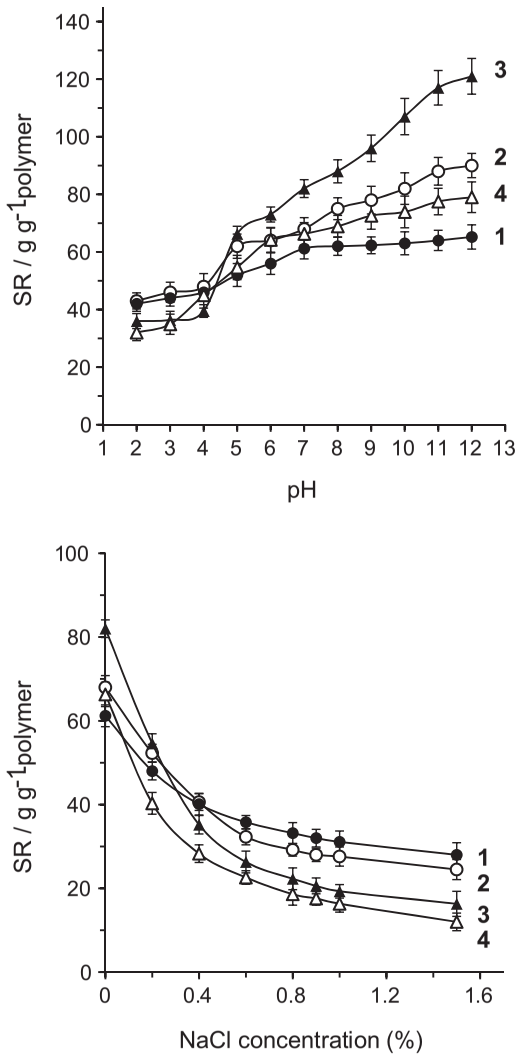

Fig. 6. Effect of (a) pH-dependency and (b) ionic strength on the swelling ratio (SR) of GG hydrogels (samples **1**–**4**).

3.6. Enzymatic degradability

GG and galactomannans are quantitatively hydrolyzed to Gal and manno-oligosaccharides by β-mannanase and α-galactosidase (Duffaud, McCutchen, Leduc, Parker, & Kelly, 1997; Moreira & Filho, 2008). The degradability of the hydrogels swollen in sodium acetate buffer (pH 4.5) was estimated using a mixture of these enzymes (Table 3). Under the conditions employed, the degradability of GG reached 65, and 65 and 64% of the blanched Gal residues and mannan backbone were hydrolyzed, respectively. In the hydrogels, the total degradabilities of samples **1**, **2**, **3**, and **4** decreased to 57, 47, 39, and 30%, respectively, indicating that the degradability depended on the n_{BTCA} of the hydrogels. In addition, the degradability of the blanched Gal residues was slightly lower than that of the mannan backbone for each GG hydrogel, suggesting that BTCA preferentially esterified the branched Gal residues rather than the mannan backbone.

3.7. Protein adsorption

The time-dependency of the protein adsorption by sample **4** at pH 7 is shown in Fig. 7(a). The molecular weight and stokes' radius of lysozyme are 14 kDa and 2.1 nm (Batas, Jones, & Chaudhuri, 1997; Bonincontro, Calandrini, & Onori, 2001), and those of BSA are 66 kDa

Table 3
Amount of Gal and Man residues in GG and GG hydrogels (samples **1**–**4**) before enzyme-degradation and as a result of the enzyme-degradability of GG and GG hydrogels.

Sample	Amount of Gal and Man residues before the enzyme degradation				Result of the enzyme degradation					
	Mw of average repeating unit[a] (g mmol^{-1})	Sum content of Gal and Man residues[b] (mmol g^{-1})	Gal contents[b] (mmol g^{-1})	Man content[b] (mmol g^{-1})	Liberated total reducing sugars[c] (mmol g^{-1})	Total degradability[c] (%)	Liberated Gal content[d] (mmol g^{-1})	Gal degradability[d] (%)	Liberated Man and Manno-oligosaccharides content[e] (mmol g^{-1})	Man degradability[e] (%)
GG	429	6.18	2.33	3.85	4.04	65	1.57	67	2.47	64
1	449	5.91	2.23	3.68	3.35	57	1.18	53	2.16	59
2	454	5.84	2.20	3.63	2.73	47	0.96	44	1.77	49
3	471	5.63	2.12	3.50	2.17	39	0.76	36	1.41	40
4	542	4.89	1.85	3.05	1.44	30	0.49	27	0.96	31

[a] One average repeating unit contained one branched Gal residue and 1.65 Man residues. Thus, the Mw of the average repeating unit of each GG hydrogel was determined by the following equation:
(Mw of average repeating unit/g mmol^{-1}) = 429 − 17 × n_{BTCA} + 260 × n_C + 299 × n_G, where n_{BTCA}, n_C, and n_G were average number of total reacted, crosslinked, and grafted BTCA molecules per one repeating unit of each GG hydrogel summarized in Table 2.

[b] Molar amount of Gal and Man residues per 1 g of GG and each GG hydrogel.

[c] Molar amount of total reducing sugars liberated from 1 g of GG or GG hydrogel by a combination of β-mannanase and α-galactosidase, which were determined by the DNS method (Miller et al., 1960). The reducing sugars were a mixture of Gal and Man residues and manno-oligosaccharaides. Degradability was determined by the following equation:
(Degradability %) = (Liberated total reducing sugars/mmol g^{-1}) × 100/(Sum amount of Gal and Man residues before the degradation/mmol g^{-1}).

[d] Gal liberated from GG or each GG hydrogel by α-galactosidase was determined according to the method previously reported (Pettersson & Pettersson, 2001). Degradability of the Gal residues was determined by the following equation:
(Degradability of Gal residues %) = (Liberated Gal/mmol g^{-1}) × 100/(Amount of Gal residues before the degradation/mmol g^{-1}).

[e] Man and manno-oligosaccharides liberated from GG or each GG hydrogel were determined by subtracting the molar amount of liberated Gal from that of the total reducing sugars. Degradability of the Man residues was determined by the following equation:
(Degradability of Man residues %) = [(Liberated total reducing sugars/mmol g^{-1}) − (Liberated Gal/mmol g^{-1})] × 100/(Amount of Man residues before the degradation/mmol g^{-1}) = [(Sum of liberated Man and Manno-oligosaccharides/mmol g^{-1})] × 100/(Amount of Man residues before the degradation/mmol g^{-1}).

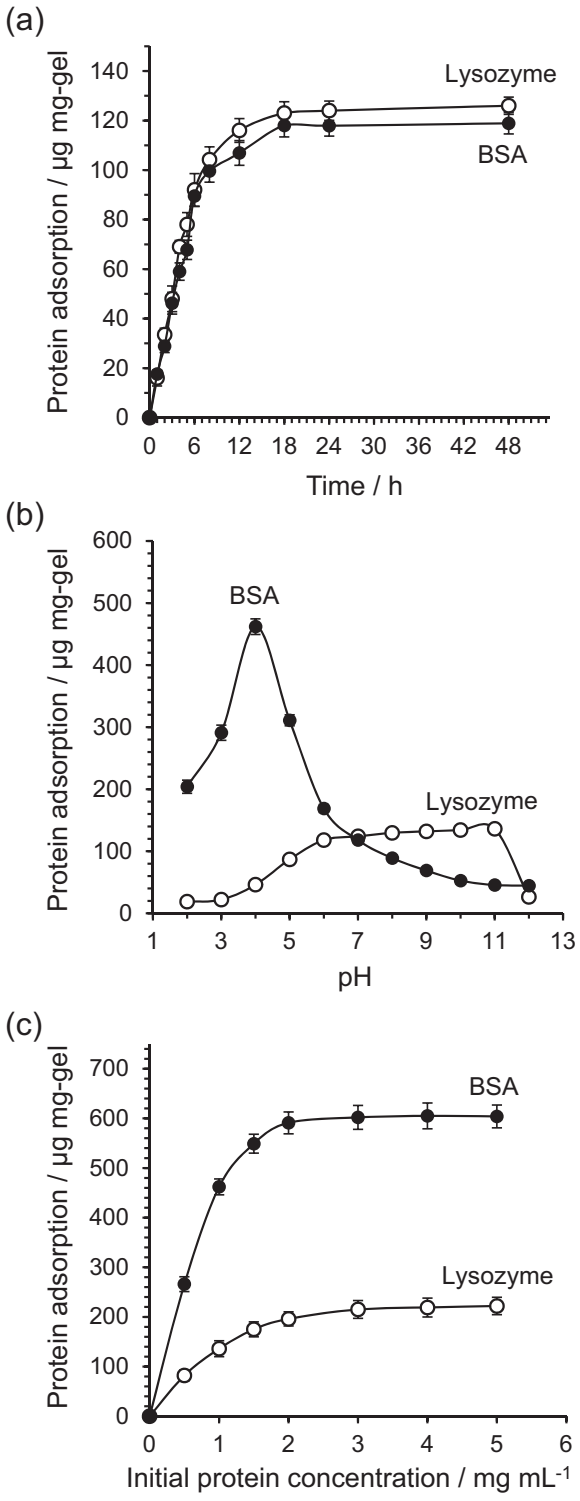

Fig. 7. Protein adsorption by GG hydrogel (sample **4**) in lysozyme- or BSA-containing buffer solutions. (a) Time-dependency of protein adsorption at pH 7.0, (b) effect of pH on protein adsorption, and (c) effect of initial protein concentration on protein adsorption in PBS buffer, pH 7.4.

and 3.4 nm (Batas et al., 1997), respectively. The adsorption of both proteins increased with increased contact time, and equilibrium was reached at about 18 h. The amount of BSA adsorbed to the hydrogel was almost the same as that of lysozyme, suggesting that the protein size and molecular weight did not affect the protein adsorption.

Fig. 7(b) shows the pH dependency of the protein adsorption after 24 h contact time. The protein adsorption of the hydrogels strongly depended on the pH of the media, and the adsorption profile of BSA was not significantly different from that of lysozyme. BSA adsorption increased in acidic media (pH 2–4), reached a maximum of 462 μg/mg at pH 4, and drastically decreased with increased pH levels up to 12. With lysozyme, the adsorption was extremely low at about 20 μg/mg-hydrogel in the pH 2–3, gradually increased at pH 3–6, was about 120–135 μg/mg in the pH region of 6–11, and decreased to 12 μg/mg at pH 12. The surface charges of proteins are negative in buffers with pH values greater than the isoelectric point (p*I*), whereas they are positive in media with pH values less than the p*I* (Denizli, Köktürk, Yavuz, & Pişkin, 1999; Denizli, Salih, & Pişkin, 1997). When the pH of the adsorption medium is approximately equal to the protein p*I*, the surface charge of the protein is electroneutral, and interactions between proteins and hydrogels are due to hydrophobic interactions (Kono, Oeda, et al., 2013). The p*I*s of lysozyme and BSA are known to be ca. 11 (Stevens, 1991) and 4.7 (Yon, 1972), respectively, and the pK_a of BTCA in GG hydrogels is 4.2. Therefore, the different adsorption profiles of lysozyme and BSA could be explained by the electrostatic and hydrophobic interactions between the proteins and the hydrogels. Specifically, when the pH of the adsorption medium was 2–3, BSA was positively charged and the carboxyl groups of the GG hydrogel were protonated, thereby lowering electrostatic interactions. At pH 4, the carboxyl groups in GG hydrogels were partially deprotonated, while the surface of BSA was oppositely charged, generating the attractive force between the two, thereby resulting in the maximum BSA adsorption. In the pH range of 5–12, the surface of BSA and the GG hydrogel were negatively charged, causing electrostatic repulsion between the two, and thus decreasing the BSA adsorption. BSA adsorption was mainly attributed to hydrophobic interactions. Similarly, in the pH 2–3, the surface of lysozyme was positively charged, and the GG hydrogels exhibited electroneutrality, indicating that the low adsorption of lysozyme was attributed to hydrophobic interactions. From pH 3–6, the carboxylic acid groups of the GG hydrogel were deprotonated, leading to the electrostatic attractive force between lysozyme and the hydrogel. From pH 6–11, electrostatic attractions between the carboxylic anion groups of GG hydrogels and the positively charged surface of lysozyme resulted in a high and constant protein adsorption. At pH 12, lysozyme and the hydrogel were charged negatively, and thus strong electrostatic repulsion occurred resulting in a drastic adsorption decrease.

Fig. 7(c) shows the effect of initial protein concentration on the protein adsorption. The adsorption of both proteins was reached an equilibrium over 3 mg mL^{-1} of initial concentrations, and the equilibrium adsorption of BSA and lysozyme was 600 μg/mg and 210 μg/mg, respectively. BSA is characterized by charged amino acids, aspartic and glutamic acids, lysine, and arginine, whereas lysozyme is not (Lewis, Snell, Hirschmann, & Fraenkel-Conrat, 1950). In addition, the charge distribution of amino acids, the amount and arrangement of hydrophobic amino acids, as well as the higher order structure of the protein may also effect the interaction between the hydrogels and the proteins (Lord, Stenzel, Simmons, & Milthorpe, 2006), which led to the difference in the adsorption.

3.8. Protein release

Fig. 8 shows the time-dependent protein release from the GG hydrogels. The release profiles of BSA and lysozyme were fast in the first hour, followed by a slow release over 24 h. In the initial release, GG hydrogels released 30–55% of the loaded proteins, which is considered to be a burst effect (Kono, Oeda, et al., 2013; Zhang et al., 2008). Thus, the hydrogel simply served as a diffusion barrier, and

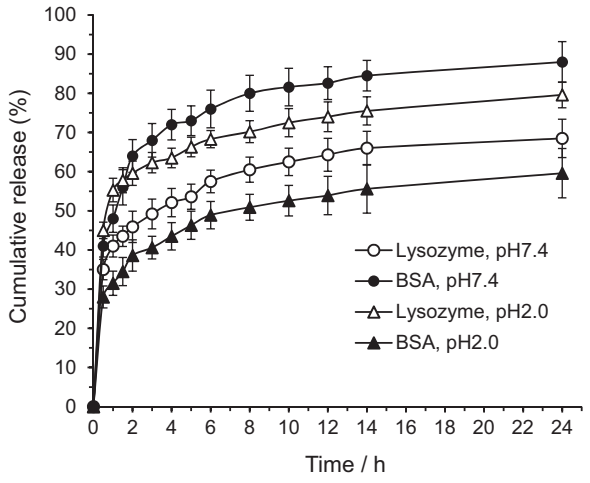

Fig. 8. Lysozyme and BSA release profile from the each protein-adsorbed GG hydrogel.

proteins were quickly released. After the initial burst, a significant amount of loaded proteins were still entrapped within the hydrogel, indicating that most of the proteins loaded into the GG hydrogel were bound to the gel network via strong interactions (Kono, Oeda, et al., 2013; Zhang et al., 2008). The remaining bound proteins were slowly released for up to 24 h after the initial burst.

The release rate of proteins slightly depended on pH; the release rate of lysozyme at pH 7.4 was slightly slower than that at pH 2.0, and the release rate of BSA at pH 7.4 was slightly higher than that at pH 2.0. It is considered that the difference is concerned with the interaction between each protein and hydrogel. As described in Section 3.7, at pH 2.0, surface charge of lysozyme was positively charged and the carboxyl groups of the GG hydrogel were protonated, thereby lowering electrostatic interactions. On the other hand, at pH 7.4, lysozyme was charged negatively and hydrogel was charged negatively, generating the attractive force between the two, thereby resulting in the slow release of lysozyme. In the case of BSA, BSA was charged positively at pH 2.0 and negatively at pH 7.4. Thus, BSA and the hydrogel were charged negatively at pH 7.4, and strong electrostatic repulsion occurred resulting in the fast release of BSA.

4. Conclusions

GG-based anionic hydrogels were prepared in a one-pot synthesis via esterification using BTCA as the crosslinking agent. The swelling behavior, rheological properties, and enzymatic degradability of the hydrogels depended on the proportion of grafted and crosslinked BTCA. The hydrogels exhibited good adsorption of BSA and lysozyme, and the protein-adsorbed GG hydrogels released the proteins in buffer solutions. The adsorbed proteins exhibited favorable drug release profiles; after an initial burst, a slow and steady release occurred. Based on these unique properties, it was concluded that the GG hydrogels have potential abilities as drug delivery carriers for protein-based drugs, although the biological safety of the GG hydrogels will need to be verified.

Acknowledgment

This work was supported in part by Grants-in-Aid for Scientific Research C-25410134 from the Japan Society for the Promotion of Science (JSPS).

References

Abo-Shosha, M. H., Ibrahim, N. A., Allam, E., & El-Zairy, E. (2008). Preparation and characterization of polyacrylic acid/karaya gum and polyacrylic acid/tamarind seed gum adducts and utilization in textile printing. *Carbohydrate Polymers*, *74*, 241–249.

Alam, N. H., Meier, R., Schneider, H., Sarker, S. A., Bardhan, P. K., Mahalanabis, D., et al. (2000). Partially hydrolyzed guar gum-supplemented oral rehydration solution in the treatment of acute diarrhea in children. *Journal of Pediatric Gastroenterology & Nutrition*, *31*, 503–507.

Argüelles-Monal, W., Goycoolea, F. M., Peniche, C., & Higuera-Ciapara, I. (1998). Rheological study of the chitosan/glutaraldehyde chemical gel system. *Polymer Gels and Networks*, *6*, 429–440.

Barth, H. G., & Smith, D. A. (1981). High-performance size-exclusion chromatography of guar gum. *Journal of Chromatography*, *206*, 410–415.

Batas, B., Jones, H. R., & Chaudhuri, J. B. (1997). Studies of the hydrodynamic volume changes that occur during refolding of lysozyme using size-exclusion chromatography. *Journal of Chromatography A*, *766*, 109–119.

Bhattarai, N., Ramay, H. R., Gunn, J., Matsen, F. A., & Zhang, M. (2005). PEG-grafted chitosan as an injectable thermosensitive hydrogel for sustained protein release. *Journal of Controlled Release*, *103*, 609–624.

Bonincontro, A., Calandrini, V., & Onori, G. (2001). Rotational and translational dynamics of lysozyme in water–glycerol solution. *Colloids and Surfaces B: Biointerfaces*, *21*, 311–316.

Brandl, F., Sommer, F., & Goepferich, A. (2007). Rational design of hydrogels for tissue engineering: Impact of physical factors on cell behavior. *Biomaterials*, *28*, 134–146.

Canet, D. (1976). Systematic errors due to improper waiting times in heteronuclear Overhauser effect measurements by the gated decoupling technique. *Journal of Magnetic Resonance*, *23*, 361–364.

Chaubey, M., & Kapoor, V. P. (2001). Structure of a galactomannan from the seeds of *Cassia angustifolia* Vahl. *Carbohydrate Research*, *332*, 439–444.

Chaurasia, M., Chourasia, M. K., Jain, N. K., Jain, A., Soni, V., Gupta, Y., et al. (2006). Cross-linked guar gum microspheres: A viable approach for improved delivery of anticancer drugs for the treatment of colorectal cancer. *AAPS PharmSciTech*, *7*, E143–E151.

Chudzikowski, R. J. (1971). Guar gum and its applications. *Journal of the Society of Cosmetic Chemists*, *22*, 43–60.

Coviello, T., Matricardi, P., Marianecci, C., & Abaique, F. (2007). Polysaccharide hydrogels for modified release formulations. *Journal of Controlled Release*, *119*, 5–24.

Crescenzi, V., Dentini, M., Risica, D., Spadoni, S., Skjak-Braek, G., Capitani, D., et al. (2004). C(6)-oxidation followed by C(5)-epimerization of guar gum studied by high field NMR. *Biomacromolecules*, *5*, 537–546.

Cui, W., Mazza, G., & Biliaderis, C. G. (1994). Chemical structure, molecular size distributions, and rheological properties of flaxseed gum. *Journal of Agricultural and Food Chemistry*, *42*, 1891–1895.

Cunha, P. L. R., Vieira, Í. G. P., Arriaga, Â. M. C., de Paula, R. C. M., & Feitosa, J. P. A. (2009). Isolation and characterization of galactomannan from *Dimorphandra gardneriana* Tul. seeds as a potential guar gum substitute. *Food Hydrocolloids*, *23*, 880–885.

Das, A., Wadhwa, S., & Srivastava, A. K. (2006). Cross-linked guar gum hydrogel discs for colon-specific delivery of ibuprofen: Formulation and in vitro evaluation. *Drug Delivery*, *13*, 139–142.

Denizli, A., Köktürk, G., Yavuz, Y., & Pişkin, E. (1999). Albumin adsorption from aqueous solutions and human plasma in a packed-bed column with Cibacron Blue F3GA-Zn(II) attached poly(EGDMA-HEMA) microbeads. *Reactive & Functional Polymers*, *40*, 195–203.

Denizli, A., Salih, B., & Pişkin, E. (1997). Comparison of metal chelate affinity sorption of BSA onto Dye/Zn(II)-derived poly(ethylene glycol dimethacrylate-hydroxyethyl methacrylate) microbeads. *Journal of Applied Polymer Science*, *65*, 2085–2093.

Duffaud, G. D., McCutchen, C. M., Leduc, P., Parker, K. N., & Kelly, R. M. (1997). Purification and characterization of extremely thermostable beta-mannanase, beta-mannosidase, and alpha-galactosidase from the hyperthermophilic eubacterium Thermotoga neapolitana 5068. *Applied and Environment Microbiology*, *63*, 169–177.

Fung, B. M., Khitrin, A. K., & Ermolaev, K. (2000). An improved broadband decoupling sequence for liquid crystals and solids. *Journal of Magnetic Resonance*, *142*, 97–101.

Gamal-Eldeen, A. M., Amer, H., & Helmy, W. A. (2006). Cancer chemopreventive and anti-inflammatory activities of chemically modified guar gum. *Chemico-Biological Interactions*, *161*, 229–240.

Gliko-Kabir, I., Yagen, B., Penhasi, A., & Rubinstein, A. (1998). Low swelling, crosslinked guar and its potential use as colon-specific drug carrier. *Pharmaceutical Research*, *15*, 1019–1025.

Gliko-Kabir, I., Yagen, B., Penhasi, A., & Rubinstein, A. (2000a). Phosphated crosslinked guar for colon-specific drug delivery. I. Preparation and physicochemical characterization. *Journal of Controlled Release*, *63*, 121–127.

Gliko-Kabir, I., Yagen, B., Penhasi, A., & Rubinstein, A. (2000b). Phosphated crosslinked guar for colon-specific drug delivery. II. In vitro and in vivo evaluation in the rat. *Journal of Controlled Release*, *63*, 129–134.

Kono, H. (2014). Characterization and properties of carboxymethyl cellulose hydrogels crosslinked by polyethylene glycol. *Carbohydrate Polymers*, *106*, 84–93.

Kono, H., Erata, T., & Takai, M. (2002). CP/MAS ^{13}C NMR study of cellulose and cellulose derivatives. 2. Complete assignment of the ^{13}C resonance for the ring carbons of cellulose triacetate polymorphs. *Journal of the American Chemical Society*, *124*, 7512–7518.

Kono, H., & Fujita, S. (2012). Biodegradable superabsorbent hydrogels derived from cellulose by esterification crosslinking with 1,2,3,4-butanetetracarboxylic dianhydride. *Carbohydrate Polymers*, *87*, 2582–2588.

Kono, H., Fujita, S., & Oeda, I. (2013). Comparative study of homogeneous solvents for the esterification crosslinking of cellulose with 1,2,3,4-butanetetracarboxylic dianhydride and water absorbency of the reaction products. *Journal of Applied Polymer Science*, *127*, 478–486.

Kono, H., Oeda, I., & Nakamura, T. (2013). The preparation, swelling characteristics, and albumin adsorption and release behaviors of a novel chitosan-based polyampholyte hydrogel. *Reactive and Functional Polymers*, *73*, 97–107.

Kono, H., Yunoki, S., Shikano, T., Fujiwara, M., Erata, T., & Takai, M. (2002). CP/MAS ^{13}C NMR study of cellulose and cellulose derivatives. 1. Complete assignment of the CP/MAS ^{13}C NMR spectrum of the native cellulose. *Journal of the American Chemical Society*, *124*, 7506–7511.

Kono, H., & Zakimi, M. (2013). Preparation, water absorbency, and enzyme degradability of novel chitin- and cellulose/chitin-based superabsorbent hydrogels. *Journal of Applied Polymer Science*, *128*, 572–581.

Leenheer, J. A., Wershaw, R. L., & Reddy, M. M. (1995). Strong-acid, carboxyl-group structures in fulvic acid from the Suwannee river, Georgia. 2. Major structures. *Environmental Science and Technology*, *29*, 399–405.

Lewis, J. C., Snell, N. S., Hirschmann, D. J., & Fraenkel-Conrat, H. (1950). Amino-acid composition of egg proteins. *Journal of Biological Chemistry*, *186*, 23–35.

Lord, M. S., Stenzel, M. H., Simmons, A., & Milthorpe, B. K. (2006). The effect of charged groups on protein interactions with poly(HEMA) hydrogels. *Biomaterials*, *27*, 567–575.

Miller, G. L., Blum, R., Glennon, W. E., & Burton, A. L. (1960). Measurement of carboxymethylcellulase activity. *Analytical Biochemistry*, *1*, 127–132.

Moreira, L. R. S., & Filho, E. X. F. (2008). An overview of mannan structure and mannan-degrading enzyme systems. *Applied Microbiology and Biotechnology*, *79*, 165–178.

Parvathy, K. S., Susheelamma, N. S., Tharanathan, R. N., & Gaonkar, A. K. (2005). A simple non-aqueous method for carboxymethylation of galactomannans. *Carbohydrate Polymers*, *62*, 137–141.

Pettersson, H., & Pettersson, G. (2001). Kinetics of the coupled reaction catalyzed by a fusion protein of β-galactosidase and galactose dehydrogenase. *Biochemica et Biophysica Acta – Protein Structure and Molecular Enzymology*, *1549*, 155–160.

Stevens, L. (1991). Egg white proteins. *Comparative Biochemistry and Physiology Part B: Comparative Biochemistry*, *100*, 1–9.

Vijayendran, B. R., & Bone, T. (1984). Absolute molecular weight and molecular weight distribution of guar by size exclusion chromatography and low-angle laser light scattering. *Carbohydrate Polymers*, *4*, 299–311.

Wang, Q., Ellis, P. R., & Ross-Murphy, S. B. (2000). The stability of guar gum in an aqueous system under acidic conditions. *Food Hydrocolloids*, *14*, 129–134.

Xu, S., Held, I., Kempf, B., Mayr, H., Steglich, W., & Zipse, H. (2005). The DMAP-catalyzed acetylation of alcohols—A mechanistic study (DMAP = 4-(dimethylamino)pyridine). *Chemistry – A European Journal*, *11*, 4751–4757.

Yon, R. J. (1972). Chromatography of lipophilic proteins on adsorbents containing mixed hydrophobic and ionic groups. *Biochemical Journal*, *126*, 765–767.

Zhang, C., Cheng, Y., Qu, G., Wu, X., Ding, Y., Cheng, Z., et al. (2008). Preparation and characterization of galactosylated chitosan coated BSA microspheres containing 5-fluorouracil. *Carbohydrate Polymers*, *72*, 390–397.